CrossMark

Induction Hardened Layer Characterization and Grinding Burn Detection by Magnetic Barkhausen Noise Analysis

Aitor Lasaosa[1] · **Kizkitza Gurruchaga[1]** · **Fernando Arizti[1]** · **Ane Martinez-De-Guerenu[1]**

Abstract The quality of the ball screw shafts used in the aeronautical sector has to be controlled and certified with the most advanced non-destructive techniques. The capacity of magnetic Barkhausen noise (MBN) as a non-destructive technique to control the quality of ball screw shafts by assuring the appropriate induction hardened layer depth and detecting local overheated regions, known as grinding burns, which may occur during grinding processes is shown in the present work. Magnetic Barkhausen noise measurements were made with a system designed and implemented by the authors and the derived parameters were compared with microhardness measurements made at various depths after the different induction hardening treatments and the grinding processes were applied. A multiparametric study of the MBN signal as a function of the magnetic field in the surface of the sample is done in order to estimate the thickness of the hardened layer and to detect the grinding burns produced during grinding processes. The hardened layer thickness can be characterized with an error of ± 200 μm in the range between 150 and 2500 μm by the position of the first peak of the MBN envelope in terms of the tangential magnetic field measured at the surface and the grinding burns can be detected with the position of the second peak of the MBN envelope in terms of the tangential magnetic field measured at the surface.

✉ Ane Martinez-De-Guerenu
   amartinez@ceit.es

   Aitor Lasaosa
   alasaosa@ceit.es

   Kizkitza Gurruchaga
   kgurruchaga@ceit.es

   Fernando Arizti
   fernando@ceit.es

[1] Ceit and Tecnun (University of Navarra), Manuel de Lardizábal 15, 20018 San Sebastián, Spain

1 Introduction

Electro-mechanical actuators (EMAs) are safety-critical components of an aerospace system where an undetected failure can lead to serious consequences. EMAs are basically equipped with a motor, a ball screw and the control electronics. In order to improve the fatigue life of the ball screw shafts, they are subjected to hardening treatment of the surface, which produces a hard and wear-resistant surface layer, while the inside of the part remains ductile. If the depth of the hardened layer, known as "case depth", is not controlled a premature failure of the ball screw shafts may occur. After the case hardening treatment, the ball screw shafts are ground to achieve the final dimensions. During grinding a non-desired local increase of the temperature can produce a defect known as grinding burn. Depending on the temperature reached during grinding, a relative increase of the tensile residual stresses, a decrease in surface hardness, or surface rehardening may occur. Any of these effects can lead to a reduction of the service life of the part [1,2]. It is therefore necessary to control both the correct hardening treatment of the surface and the correct grinding of the workpiece at 100% of production with a non-destructive testing (NDT) technique.

Magnetic Barkhausen noise (MBN) was selected as a quality control NDT technique due to its high sensitivity to changes in microstructure [3–18] and residual stresses [3,4,6–12,14,15,18] on the surface of ferromagnetic parts. MBN is an electromagnetic technique consisting of the study of the signal produced by the movement of the magnetic domain walls inside ferromagnetic materials when a time-

🙋 Springer

varying magnetic field is applied. In general terms, a decrease in hardness increases the MBN signal amplitude and shifts the peak position of the envelope of MBN to lower levels of the applied field; while an increase in the hardness decreases the peak amplitude and moves the position of the peak towards higher levels of the applied field [3–7]. Similarly, tensile stresses induce an increase in the amplitude of the MBN, while compressive stresses decrease it [6,9–11,15]. However, it has been reported that the position of the peak is less sensitive to the variation in residual stresses [9,14]. This technique is especially useful for the characterization of these properties in the surface region between a few tens of micrometers [18] and a few millimeters [3–6,9,12]. Due to these characteristics, it has been observed that the MBN signal can be used successfully to detect grinding burns and to identify the intensity level of the grinding burns [10,15].

On the other hand, different microstructural phases produce different Barkhausen signals. For example, ferrite microstructures produce a strong Barkhausen activity located at low magnetic fields, in contrast to martensite microstructures, which have low Barkhausen emission located at high fields. Therefore, if the material comprises two different phases, the MBN signal's envelope can present a shape with two peaks [3,4,6–9,12]. In surface hardened components, where two layers of different phases are present (martensite in the outer layer and ferrite, pearlite or bainite phases in the core), if the outer layer is not too big and a high enough magnetic field is applied, MBN information from both layers reaches the MBN sensor located at the surface and then the MBN envelope presents a two-peak shape. The first peak, at lower applied voltage, is attributed to the magnetization in the softer core [3,4,9] or to the transition zone between the hardened surface and the softer core [5,6,12], and the second peak occurring at higher applied voltage is attributed to the magnetization in the harder near-surface layers. Depending on the hardness of both phases and the distance from the surface to the core material it is also possible to have overlapping peaks instead of separated ones [9]. In this sense, it has been observed that the amplitude of the first peak decreases gradually with the increase in the depth of the hardened layer (case depth) up to a certain depth of the hardened layer, where the first peak disappears [4,6,15,16]. This is explained by the fact that MBN that passes through a ferromagnetic material is attenuated mainly due to eddy current damping [3,4,7,8,12,19–21]. As a consequence, the amplitude of MBN is governed by the following equation:

$$MBN(x) = MBN_0 \exp^{-x/\delta}, \tag{1}$$

where MBN_0 is the amplitude of the MBN signal emitted at its origin, x is the distance to the surface from the origin of the signal, $MBN(x)$ is the value of the MBN coming from distance x from the surface, and δ is the skin depth of the MBN signal calculated as:

$$\delta = \sqrt{\frac{1}{\pi \sigma \mu f}}, \tag{2}$$

where σ is the electrical conductivity of the material, μ is the absolute magnetic permeability of the material and f is the frequency of the MBN signal emitted.

The applied magnetic field is also attenuated as it passes through the ferromagnetic material, not only because of eddy current damping but also because of magnetic viscosity, demagnetization and other effects [9,17,19]. Due to the many effects present, there is no equation that models this attenuation, but it has been reported that the deeper the magnetic field penetrates, the more it will be attenuated [9,17,19]. Hence, in order to apply a certain magnetic field value at the material at a greater depth, it is necessary to apply a higher magnetic field on the surface than for the material located at smaller depth. However, the attenuation of the applied magnetic field has not been considered in the characterization of case depth previously in the literature.

In the present work a multiparametric study of the MBN signal is carried out in order to simultaneously characterize the case depth of induction hardened ball screw shafts and to detect possible grinding burns with a single MBN measurement. Additionally, the characterization of the case depth is done by considering the attenuation of both the applied magnetic field and the emitted MBN signal.

2 Experimental Procedure

In order to study the sensitivity of the MBN technique in characterizing the induction hardened layer depth and grinding burns, several ball screw shafts of 10 mm in diameter and with a threaded length of 60 mm were machined and heat treated by applying different induction hardening treatments to the surface. Most of the ball screw shafts were ground in normal conditions, but in order to study the capacity to detect grinding burns, two different induction hardening treatments (T3 and T12) were selected, and some ball screw shafts were ground in normal conditions (OK) and for others grinding conditions were changed in order to artificially generate grinding burns (Not OK). The feed speed, the grinding depth and the amount of oil used as coolant were modified.

MBN measurements were performed using a system built in the laboratories of the Ceit research center in collaboration with the company Korta S.A. The excitation was produced with a programmable function generator, a power amplifier and an electromagnetic yoke made of a ferromagnetic U core and a winding designed specifically to be adapted

Fig. 1 Hardness profiles obtained in a subgroup of the normally ground ball screw shafts
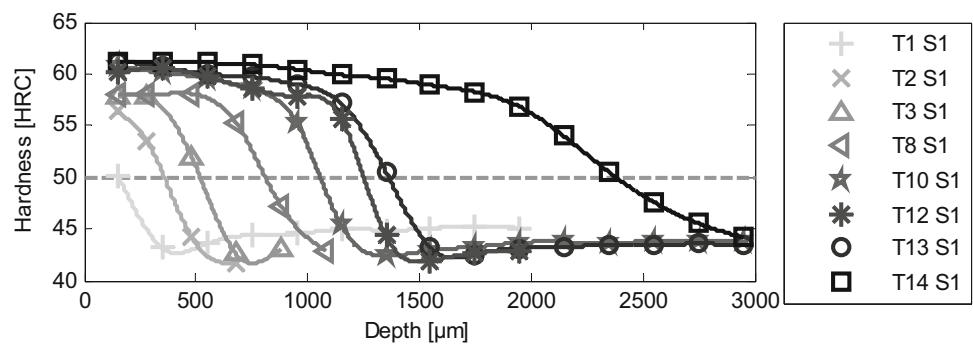
to the geometry of the ball screw shaft. Medium frequency magnetization, whose amplitude is sufficient to generate a MBN signal from the hard material of the surface, was used. The induced electromotive force signal was measured with a pick up coil placed above the surface of the sample, and after filtering the low frequencies the MBN signal was obtained and its envelope was calculated by moving root mean square (RMS). The tangential magnetic field at the surface (H_t) of the ball screw shaft was measured by a Honeywell SS495A1 solid state Hall effect sensor placed above the surface of the sample. The MBN envelope and the H_t signals were stored in a PC where they were processed. One cycle was acquired every 1 mm along the helical path of the ball screw shaft. Each cycle contains two MBN envelopes (the positive (from $-H_{tmax}$ to $+H_{tmax}$) and negative (from $+H_{tmax}$ to $-H_{tmax}$) branches of the excitation signal). The MBN envelopes and the H_t signals were averaged every 12 cycles. And from these averaged MBN envelopes and H_t signals the parameters studied in the following sections were derived and these will be referred as processed parameters.

After taking the MBN measurements, Vickers microhardness measurements were made on all the samples. They were performed with a load of 1 kg in a shallow depth of 150 μm to characterize the surface and every 200 μm at greater depths in order to characterize the hardened layer. The case depth was defined as the depth at which hardness falls below 50 HRC [22]. The equivalent approximate Rockwell C hardness was calculated according to the ASTM—E140 [23] standard.

3 Results and Discussion

3.1 Microhardness Measurements

For the sake of clarity, first the Vickers microhardness measurement data are shown, despite having been taken after the MBN measurements were performed. The surface hardness values and the case depths for each ball screw shaft are presented in Table 1 together with the grinding conditions. Figure 1 shows the hardness profiles obtained in a subgroup of the normally ground ball screw shafts after different induc-

Table 1 List of samples used in the present study, showing the number of heat treatment and sample and the grinding conditions

Heat treatment and sample	Grinding conditions	Surface hardness (HRC)	Case depth (μm)
T1 S1	OK	50	150
T2 S1	OK	56	358
T3 S1	OK	58	519
T4 S1	OK	60	616
T5 S1	OK	60	661
T6 S1	OK	59	797
T7 S1	OK	58	799
T8 S1	OK	58	810
T9 S1	OK	60	812
T10 S1	OK	61	1056
T11 S1	OK	59	1152
T12 S1	OK	60	1250
T13 S1	OK	61	1361
T14 S1	OK	61	2383
T3 S2	Not OK	57	473
T12 S2	Not OK	54	1190
T12 S3	Not OK	59	1210

Surface hardness and case depth values for the ball screw shafts obtained from microhardness measurements. Surface hardness is measured at 150 μm and case depth is considered as the depth at which the hardness falls below 50 HRC

tion hardening treatments. It can be seen that ball screw shaft T1 S1 presents the lowest case depth and much lower surface hardness (50 HRC) compared with the other samples' surface hardness (56 HRC–61 HRC) which is due to an incomplete heat treatment. Ball screw shaft T14 S1 presents a much higher case depth (2383 μm) compared with the other samples' case depth (150–1361 μm).

The hardness profiles obtained in the ball screw shafts that were abnormally ground (Not OK) are shown in Fig. 2 together with the profiles of the ball screw shafts ground in normal conditions (OK) from the same induction hardening treatments (T3 and T12). The ball screw shaft T3 S1 (OK) shows a hardness of HRC 58, when the ball screw shaft T3 S2 (Not OK) presents a surface hardness of 57 HRC and

Fig. 2 Hardness profiles of the normally and abnormally ground ball screw shafts from heat treatments T3 and T12
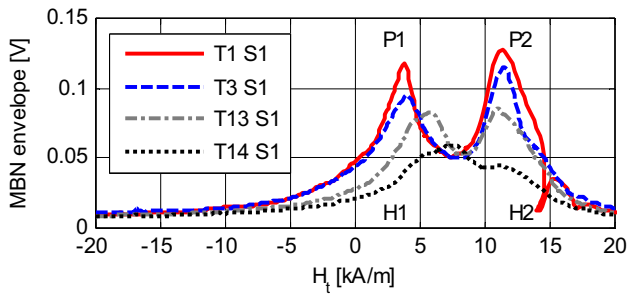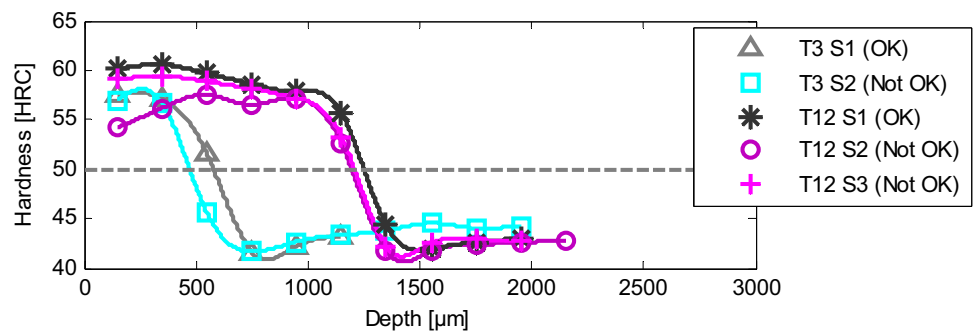
Fig. 3 MBN envelope signal as a function of the tangential magnetic field (H_t) measured on the surface of a representative point of ball screw shafts machined in normal conditions

ball screw shafts T12 S1 (OK) has a surface hardness of 60 HRC, when the ball screw shafts T12 S2 (Not OK) and T12 S3 (Not OK) have a surface hardness of 54 HRC and 59 HRC respectively. Additionally, it is observed that the case depth in the burned shafts does not change significantly with respect to the normally ground ball screw shafts for each heat treatment.

3.2 Case Depth Characterization by MBN

Figure 3 shows the MBN envelope as a function of the tangential magnetic field at the surface of the sample (H_t) obtained on a representative point of normally ground ball screw shafts T1 S1, T3 S1, T13 S1 and T14 S1. It can be seen that the envelope of the MBN signal shows two distinct peaks. The first peak provides information about the softer core material while the second peak gives information about the surface material, which is harder after induction hardening treatment [3–6,9,12]. These peaks were parametrized by their amplitudes (P1 and P2) and their positions in terms of H_t(H1 and H2) as is shown in Fig. 3. Ball screw shaft T1 S1 presents the largest P1 and the lowest H1 values and ball screw shaft T14 S1 presents the lowest P1 and the highest H1 values. The other ball screw shafts present intermediate values according to their case depths, i.e. their P1 decreases and their H1 increases as the case depth increases from ball screw shaft T1 to ball screw shaft T14. At the same time, P2 decreases in the samples as the case depth increases, in the same way as

with P1 and H2 presents similar values for all the ball screw shafts.

It should be noted that the MBN envelope of the ball screw shaft T14 S1 presents a two peak shape despite its large case depth (see Fig. 1; Table 1). In general terms, the information from the first peak comes from the core phase present in the transition zone [5,6,12] or in the core [3,4,9]. In ball screw shaft T14 S1 both of them are located at a depth greater than 1500 μm. The T13 S1 is the ball screw shaft with the second largest case depth, which is smaller than 1500 μm (Fig. 1). Therefore, in ball screw shafts from T1 S1 to T13 S1, the MBN signal from the first peak can be interpreted as coming from the core, not just from the transition zone.

To study the case depth in the ball screw shafts in production the parameters considered were the amplitudes of the two peaks (P1 and P2), the relation between these amplitudes (P2/P1) and the position of the amplitude of first peak in terms of H_t(H1). The H2 parameter was not considered due to the little difference shown between the heat treatments shown in Fig. 3. In Fig. 4a–d the parameters P1, P2, P2/P1 and H1 for each ball screw shaft are shown as a function of their case depth, respectively. The points shown in the figures are the average values of the processed values of P1, P2, P2/P1 and H1 along the helical length. The error bars on each average point represent the standard deviation of these measurements. Note the small scatter of the four parameters along the whole thread of the shafts for the whole set of induction heat treatments applied, especially on H1.

As the case depth decreases higher values of P1 (Fig. 4a) are obtained, which can be explained by taking into consideration that the attenuation due to eddy current damping suffered by the MBN signal [18–21] emitted from the core material is smaller as the MBN signal crosses through a smaller thickness of material to reach the surface MBN sensor [3–5,9,12]. Although an inverse linear trend is observed between the P1 values and the case depth, the scatter of P1 values in ball screw shafts with similar case depth would yield with the regression shown in the figure an error greater than ±500 μm in the case depth estimation. This makes the use of this parameter impractical to characterize the case depth with adequate precision. The high scatter of the peak amplitudes for similar case depths has been shown before by other
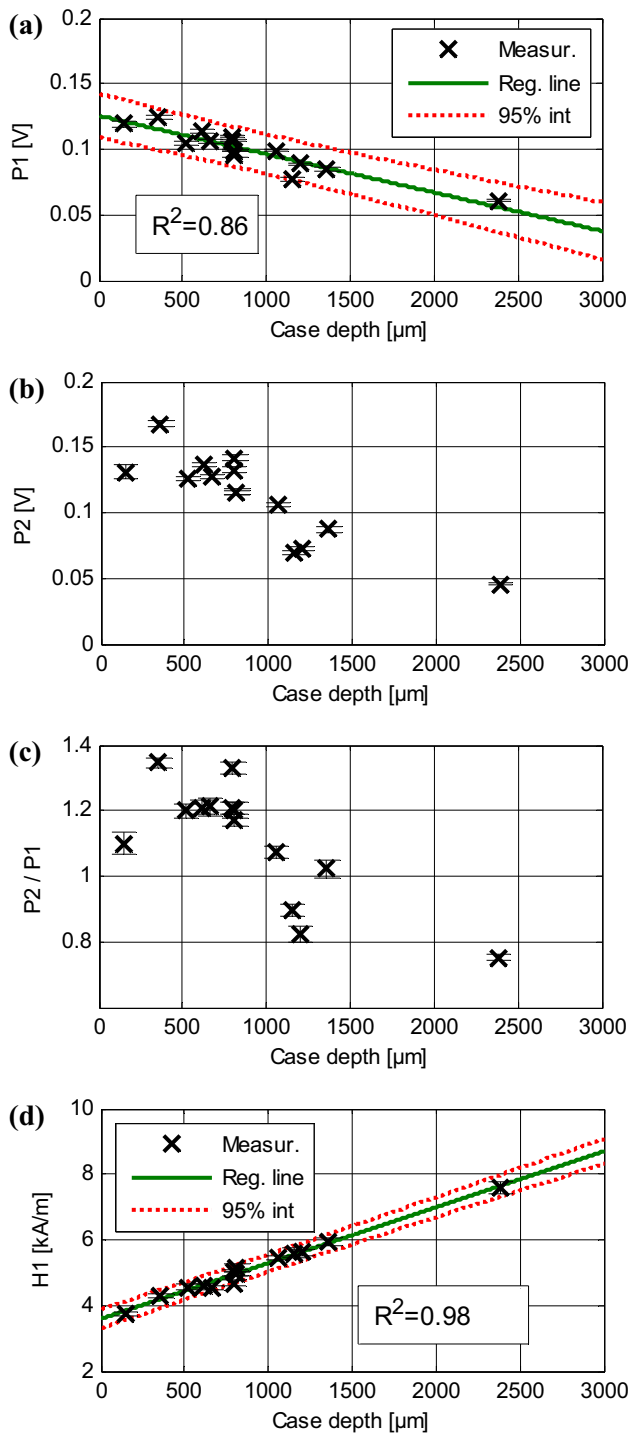
Fig. 4 Average values of parameters **a** P1, **b** P2, **c** P2/P1, **d** H1 throughout the useful length of the thread in the screw shafts machined in normal conditions (x *marker*) with its standard deviation (*error bars*). In **a**, **d** linear regression line (*continuous line*) and *upper* and *lower* 95% confidence bounds (*dotted lines*) are shown
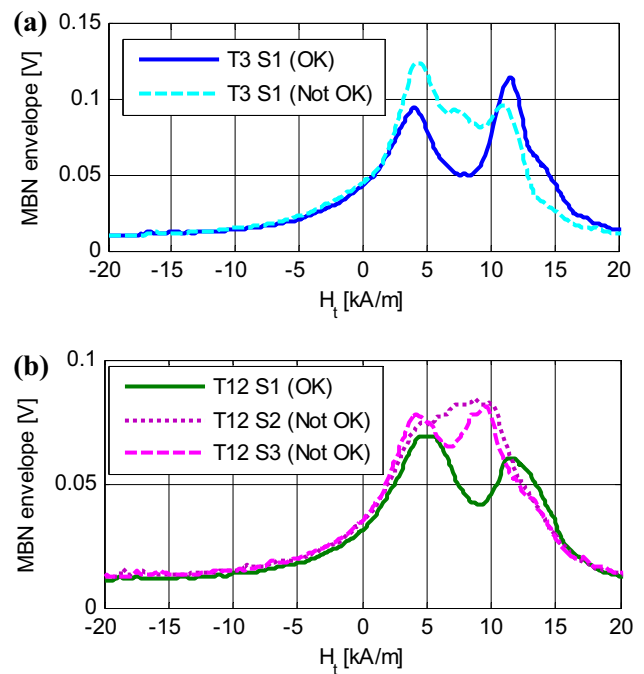
Fig. 5 Envelope of the MBN signal as a function of the tangential magnetic field (Ht) measured on the surface of a representative point of the ball screw shafts ground in normal and abnormal conditions for heat treatments **a** T3 and **b** T12

the amplitude of the second peak (P2) is shown. In this case the relationship between the P2 parameter and the case depth value is even poorer, as this parameter is influenced by the case depth [3–5,12], the surface hardness [16] and residual stresses [3,4,6,9,12,15], that can have effects on the parameter in opposite directions. The relation between P2 and P1 is presented in Fig. 4c). Although this relationship has been reported to show the best correlation coefficients within these three parameters in the literature [3–5], in the present case it shows the worse correlation coefficient as combining two parameters with high scatter only increases the dispersion.

In Fig. 4d it can be seen that H1 increases linearly as the case depth increases. This may be explained by considering the attenuation of the magnetic field. As the applied magnetic field is attenuated when penetrating through the ferromagnetic material [9,17,19], if the core is at a greater distance from the surface, it is necessary to apply a higher magnetic field to the surface in order to achieve the same level of magnetic field necessary to generate the peak of the envelope coming from the core material. The peak position was also analyzed previously by other authors, but instead of considering the position of the peak in terms of the tangential magnetic field, the position was determined as a function of the magnetizing current [9] and no relationship between this parameter and the case depth was found. The main reason of the difference between the actual measurement of the tangential magnetic field on the surface and the applied current

authors [3,4,9,15] and it was attributed to the high sensitivity of the peak height to residual stresses present in the material after heat treatment or manufacturing. In Fig. 4 b)
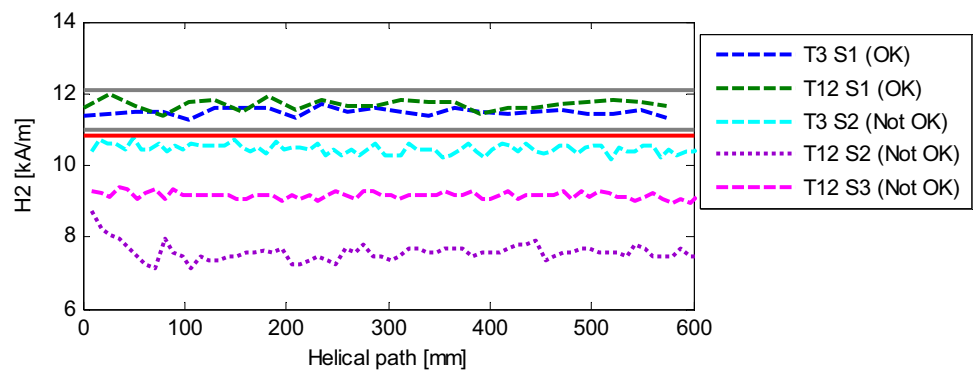
Fig. 6 Evolution of the H2 parameter along the helical path in normally and abnormally ground ball screw shafts. The maximum and minimum value of H2 parameter of the normally ground ball screw shafts (*OK*) are plotted in *continuous light gray lines* and the threshold between *OK* and *Not OK* ball screw shafts is plotted as *continuous dark line (red in online version)*

is that their relationship is influenced by the magnetic distortion, studied recently by Moorthy [24], and according to this, the relationship is influenced by the permeability of the sample, which varies with the case depth, making the magnetic field to be differently distorted as a function of the case depth.

Moreover, the H1 parameter presents a very low scatter and as a consequence it is possible to estimate the case depth with only an error of around $\pm 200\,\mu m$. The difference with the large scatter present in the parameter P1 is the low or negligible effect that residual stresses have on the position of the peak (H1) while the amplitude of the peak is very sensitive to changes on stress level [6].

3.3 Grinding Burn Characterization by MBN

In Fig. 5a, b the MBN envelopes as a function of the tangential magnetic field at the surface of the sample (H_t) obtained on a representative point of the helical path of the ball screw shaft thread for the normally ground (OK) samples and for the abnormally ground ones, with grinding burns (Not OK), are shown for the T3 and T12 heat treatments, respectively. It is noted that regardless of the heat treatment there is no direct relationship between the intensity of the grinding burn and the amplitudes of the peaks or the position of the first peak. However, the position of the second peak (H2) of the ball screw shafts with grinding burn moves toward lower values of H_t and the amplitude of the envelope between the two peaks increases, leading to a shape of a unique peak in the ball screw shaft that has undergone the most severe grinding burn (T12 S3, see Fig. 2). This is the result of the merge of the first peak and the second peak due to the displacement of the second peak to lower fields as a consequence of the reduction of surface hardness which shifts the peak to a lower value of magnetic field [16]. The same effect can also happen when the core material is so far away, that the first peak moves too near to the second peak coming from the surface [9]. Here the unique peak is used as the second peak for the parameterization when identifying the grinding burns. Hence, the parameter H2 can be used to separate the ball

screw shafts with grinding burns from those ground in normal conditions.

The processed H2 parameter obtained along the helical length of the thread in the selected ball screw shafts from the heat treatments T3 and T12 is shown in Fig. 6. The horizontal continuous gray lines indicate the maximum and minimum values of the processed H2 parameter for the whole set of normally ground (OK) ball screw shafts (Table 1). For the normal grinding conditions, the H2 parameter is not greatly influenced by the different heat treatments or surface hardness as all measurements are in the small range of H2 limited by the gray lines. However, the processed H2 moves to lower values of the H_t in the ball screw shafts that have undergone grinding burns independently of their surface hardness or case depth. Therefore, the selection of control thresholds for this parameter (shown as horizontal continuous red line in Fig. 6) distinguish all the OK ground ball screw shafts from those that have a grinding burn.

4 Conclusions

In the present work the characterization of the case depth after the induction hardening of the surface and the quality assurance that the part has not undergone a grinding burn have been achieved through a unique non-destructive method of measurement.

It has been demonstrated that the position of the first peak in terms of the magnetic field, H1, derived from the envelope of MBN is linearly related with the case depth in the range between 150 and $2500\,\mu m$ and that it could be used to characterize the case depth non-destructively with an accuracy slightly smaller than $\pm 200\,\mu m$. Therefore, this allowed the implementation of a non-destructive quality control system in order to ensure that 100% of the ball screw shafts have the necessary case depth.

Working with only one of the parameters derived from the envelope of MBN, the position of the second peak, H2, it can be determined whether a screw shaft has undergone a grinding burn independently of the depth of the hard surface layer.

Therefore, by performing a single measurement of MBN and a multiparametric study of the MBN envelope, it is possible to estimate the case hardening depth and detect possible grinding defects in any region of the thread of the ball screw shafts.

References

1. Grum, J.: A review of the influence of grinding conditions on resulting residual stresses after induction surface hardening and grinding. J. Mater. Process. Technol. **114**, 212–226 (2001). doi:10.1016/S0924-0136(01)00562-3

2. Savaria, V., Monajati, H., Bridier, F., Bocher, P.: Measurement and correction of residual stress gradients in aeronautical gears after various induction surface hardening treatments. J. Mater. Process. Technol. **220**, 113–123 (2015). doi:10.1016/j.jmatprotec.2014.12.009

3. Bach, G., Goebbels, K., Theiner, W.A.: Characterization of hardening depth by Barkhausen noise measurement. Mater. Eval. **46**, 1576–1580 (1988)

4. Saquet, O., Tapuleasa, D., Chicois, J.: Use of Barkhausen noise for determination of surface hardened depth. Nondestr. Test. Eval. **14**, 277–292 (1998). doi:10.1080/10589759808953055

5. Vaidyanathan, S., Moorthy, V., Jayakumar, T., Raj, B.: Evaluation of induction hardened case depth through microstructural characterisation using magnetic Barkhausen emission technique. Mater. Sci. Technol. Ser. **16**, 202–208 (2000). doi:10.1179/026708300101507550

6. Moorthy, V., Shaw, B.A., Day, S.: Evaluation of applied and residual stresses in case-carburised En36 steel subjected to bending using the magnetic Barkhausen emission technique. Acta Mater. **52**, 1927–1936 (2004). doi:10.1016/j.actamat.2003.12.034

7. D'Amato, C., Verdu, C., Kleber, X., Regheere, G., Vincent, A.: Characterization of austempered ductile iron through Barkhausen noise measurements. J. Nondestr. Eval. **22**, 127–139 (2003). doi:10.1023/B:JONE.0000022032.66648.c5

8. Kleber, X., Hug, A., Merlin, J., Soler, M.: Ferrite-martensite steels characterization using magnetic Barkhausen noise measurements. ISIJ Int. **44**, 1033–1039 (2004). doi:10.2355/isijinternational.44.1033

9. Blaow, M., Evans, J.T., Shaw, B.A.: Effect of hardness and composition gradients on Barkhausen emission in case hardened steel. J. Magn. Magn. Mater. **303**, 153–159 (2006). doi:10.1016/j.jmmm.2005.07.034

10. Bahadur, A., Mitra, A., Kumar, R.B., Sagar, P.S.: Evaluation and correlation of residual stress measurement in steel. J. Nondestr. Eval. **26**, 47–55 (2007). doi:10.1007/s10921-007-0019-8

11. Davut, K., Gur, H.C.: Monitoring the microstructural changes during tempering of quenched SAE 5140 steel by magnetic Barkhausen noise. J. Nondestr. Eval. **26**, 107–113 (2007). doi:10.1007/s10921-007-0025-x

12. Moorthy, V., Shaw, B.A.: Magnetic Barkhausen emission measurements for evaluation of material properties in gears. J. Test. Eval. **23**, 317–347 (2008). doi:10.1080/10589750802275980

13. Gurruchaga, K., Martínez-De-Guerenu, A., Soto, M., Arizti, F.: Magnetic Barkhausen noise for characterization of recovery and recrystallization. IEEE T Magn. **46**, 513–516 (2010). doi:10.1109/TMAG.2009.2029069

14. Santa-aho, S., Vippola, M., Sorsa, A., Latokartano, J., Lindgren, M., Leiviskä, K., et al.: Development of Barkhausen noise calibration blocks for reliable grinding burn detection. J. Mater. Process. Technol. **212**, 408–416 (2012). doi:10.1016/j.jmatprotec.2011.10.003

15. Santa-aho, S., Vippola, M., Sorsa, A., Leiviskä, K., Lindgren, M., Lepistö, T.: Utilization of Barkhausen noise magnetizing sweeps for case-depth detection from hardened steel. NDT&E Int. **52**, 95–102 (2012). doi:10.1016/j.ndteint.2012.05.005

16. Franco, F.A., Gonzalez, M.F.R., De Campos, M.F., Padovese, L.R.: Relation between magnetic Barkhausen noise and hardness for Jominy Quench tests in SAE 4140 and 6150 steels. J. Nondestr. Eval. **32**, 93–103 (2013). doi:10.1007/s10921-012-0162-8

17. Vashista, M., Moorthy, V.: On the shape of the magnetic Barkhausen noise profile for better revelation of the effect of microstructures on the magnetisation process in ferritic steels. J. Magn. Magn. Mater. **393**, 584–592 (2015). doi:10.1016/j.jmmm.2015.06.008

18. Stupakov, A., Neslusan, M., Perevertov, O.: Detection of a milling-induced surface damage by the magnetic Barkhausen noise. J. Magn. Magn. Mater. **410**, 198–209 (2016). doi:10.1016/j.jmmm.2016.03.036

19. Jiles, D.C.: Magnetization and magnetic moment. In: Jiles, D.C. (ed.) Introduction to Magnetism and Magnetic Materials, 2nd edn, pp. 57–60. Chapman & Hall, Boca Raton (1998)

20. Kypris, O., Nlebedim, I.C., Jiles, D.C.: A model for the Barkhausen frequency spectrum as a function of applied stress. J. Appl. Phys. **115**, 083906 (2014). doi:10.1063/1.4866195

21. Lasaosa, A., Gurruchaga, K., Garcia, V.N., Martinez-de-Guerenu, A.: Characterisation of in-depth stress state by magnetic Barkhausen noise on machined steel acquiring different frequency bands. Adv. Mater. Res. **996**, 373–379 (2014). doi:10.4028/www.scientific.net/AMR.996.373

22. Haimbaugh, R.E.: Induction heat treating process analysis. In: Haimbaugh, R.E. (ed.) Practical Induction Heat Treating, 2nd edn, p. 225. ASM International, New York (2015)

23. ASTM E 140: Standard Hardness Conversion Tables for Metals Relationship among Brinell Hardness, Vickers Hardness, Rockwell Hardness, Superficial Hardness, Knoop Hardness, Scleroscope Hardness, and Leeb Hardness (2007)

24. Moorthy, V.: Unique correlation between non-linear distortion of tangential magnetic field and magnetic excitation voltage—unexplored ferromagnetic phenomena and their application for ferromagnetic materials evaluation. J. Magn. Magn. Mater. **398**, 101–108 (2016). doi:10.1016/j.jmmm.2015.09.029